esa
European Space Agency

Sea Ice Climate Change Initiative: Phase 1

ANT D1.3 Product User Guide (PUG)

This PUG is for Antarctic AMSR-E snow depth product SD v1.1

Doc Ref: SICCI-ANT-SD-PUG-14-08

Version: 2.1

Date: 05 May 2015

NERSC

Consortium Members

CGI · Meteorologisk institutt met.no · DTU · UCL · FMI · Ifremer · Max-Planck-Institut für Meteorologie · DMI Vejr, klima og hav · AWI · Universität Hamburg DER FORSCHUNG | DER LEHRE | DER BILDUNG · UNIVERSITY OF CAMBRIDGE · Universität Bremen

Change Record

Issue	Date	Reason for Change	Author(s)
1.0	05 December 2014	First Issue to be provided together with ANT-SIT-Option Snow Depth product SDv1.0	Stefan Kern, Torben Frost
1.1	09 December 2014	Final issue	Stefan Kern, Torben Frost, Georg Heygster
2.0	30 April 2015	Final issue for ANT-SIT-Option Snow Depth product SDv1.1	Stefan Kern, Torben Frost, Georg Heygster

Authorship

Role	Name	Signature
Written by:	Stefan Kern, Torben Frost, Georg Heygster	
Checked by:		
Approved by:		
Authorised by:		

Distribution

Organisation	Names	Contact Details
ESA	Pascal Lecomte	Pascal.Lecomte@esa.int
NERSC	Stein Sandven	Stein.Sandven@nersc.no
CGI (previously Logica)	Gary Timms, Ed Pechorro	gary.timms@cgi.com; ed.pechorro@cgi.com;
AWI	Sandra Schwegmann, Marcel Nicolaus	sandra.schwegmann@awi.de, marcel.nicolaus@awi.de
FMI	Eero Rinne	eero.rinne@fmi.fi
University of Hamburg	Stefan Kern	stefan.kern@zmaw.de;
University of Bremen	Georg Heygster, Torben Frost	heygster@uni-bremen.de, frosttorben@googlemail.com
University of Cambridge	Peter Wadhams	pw11@cam.ac.uk

Table of Contents

1 Introduction

1.1 Document Structure

This document describes the dataset for the Sea Ice ECV project produced in Phase 1 of ESA's Climate Change Initiative – Antarctic Sea Ice Thickness Option.

1.2 Document Status

This is the 1st issue of the PUG document for the Antarctic Sea Ice Thickness option snow depth product.

1.3 Reference Documents and Datasets

Acronym	Title	Reference	Issue
RD-01	ANT D1.1 Passive Microwave Snow Depth on Antarctic sea ice assessment.	Frost, T., G. Heygster, and S. Kern, SICCI-ANT-SD-PUG-14-08	v1.0 Nov. 2014
RD-02	ANT D1.2 Antarctic Snow Depth from Alternative Sources	Kern, S., SICCI-ANT-SD-PUG-14-08	v1.0 Nov. 2014
RD-03	D3.4 Product User Guide (PUG)	Lavergne, T., and E. Rinne, SICCI-PUG-13-07	v2.0 Aug. 2014
RD-04	Snow depth distribution over sea ice in the southern ocean from satellite passive microwave data	Markus, T., and D. J. Cavalieri, Antarctic Sea Ice: Physical Processes, Interactions, and Variability, M. O. Jeffries (Ed.), AGU Antarctic Research Series, vol. 74, pp. 19-39, 1998	n.a.
RD-05	Sea ice concentration, ice temperature, and snow depth using AMSR-E data	Comiso, J. C., D. J. Cavalieri, and T. Markus, IEEE Transactions on Geoscience and Remote Sensing, 41(2), 243-252, 2003	n.a.
RD-06	Algorithm Theoretical Basis Document: Sea Ice Products	Markus, T., D. J. Cavalieri, and A. Ivanoff, Technical Report, Cryospheric Sciences Laboratory, NASA Goddard Space Flight Center, Greenbelt, MD 20771, 2011a.	Dec. 2011
RD-07	Comparison of SSM/I and AMSR-E sea ice concentrations with ASPeCt ship observations around Antarctica	Beitsch, A., S. Kern, and L. Kaleschke, IEEE Transaction on Geoscience and Remote Sensing, 53(4), 10.1109/TGRS.2014.2351497, 2015.	n.a.

Acronym	Title	Reference	Issue
RD-08	Evaluation of AMSR-E snow depth product over East Antarctic sea ice using in situ measurements and aerial photography	Worby, A. P., T. Markus, A. D. Steer, V. I. Lytle, and R. A. Massom, Journal of Geophysical Research, 113, C05S94, doi:10.1029/2007JC004181, 2008b	n.a.
RD-09	Microwave Signatures of Snow on Sea Ice: Observations	Markus, T., D. J. Cavalieri, A. J. Gasiewski, M. Klein, J. A. Maslanik, D. C. Powell, B. B. Stankov, J. C. Stroeve, and M. Sturm, IEEE Transactions on Geoscience and Remote Sensing, 44(11), 3081-3090, doi: 10.1109/TGRS.2006.883134, 2006a.	n.a.
RD-10	Intercomparisons of Antarctic sea ice types from visual ship, RADARSAT-1 SAR, Envisat ASAR, QuikSCAT, and AMSR-E satellite observations in the Bellingshausen Sea,	Ozsoy-Cicek, B., S. Kern, S. F. Ackley, H. Xie, and A. E. Tekeli, Deep-Sea Research, part II, 58(9-10),1092-1111, doi:10.1016/j.dsr2.2010.10.031, 2011	n.a.
RD-11	An intercomparison between AMSR-E snow depth and satellite C- and Ku-Band radar backscatter data for Antarctic sea ice,	Kern, S., B. Ozsoy-Cicek, S. Willmes, M. Nicolaus, C. Haas, and S. F. Ackley, Annals of Glaciology, 52(57), 279-290, 2011	n.a.
RD-12	Winter snow cover variability on East Antarctic sea ice	Massom, R. A., V. I. Lytle, A. P. Worby, and I. Allison, Journal of Geophysical Research, 103(C11), 24,837–24,855, 1998	n.a.
RD-13	Winter snow cover on sea ice in the Weddell Sea	Massom, R. A., M. R. Drinkwater, and C. Haas, Journal of Geophysical Research, 102(C1), 1101–1117, 1997	n.a.
RD-14	The thickness distribution of sea ice and snow cover during late winter in the Bellingshausen and Amundsen Seas, Antarctica	Worby, A. P., M. O. Jeffries, W. F. Weeks, K. Morris, and R. Jana, Journal of Geophysical Research, 101(C12), 28,441–28,455, 1996	n.a.
RD-15	A description of the snow cover on the winter sea ice of the Amundsen and Ross Seas	Sturm, M., K. Morris, and R. A. Massom, Antarctic Journal of the US, 30(1-4), 21-24, 1995	n.a.
RD-16	Characteristics and distribution patterns of snow and meteoric ice in the Weddell Sea and their contribution to the mass balance of sea ice	Eicken, H., M. A. Lange, H.-W. Hubberten, and P. Wadhams, Annals Geophysicae, 12, 80-93, 1994	n.a.

Acronym	Title	Reference	Issue
RD-17	Sea-ice– and snow–thickness distributions in late winter 1993 and 1994 in the Ross, Amundsen, and Bellingshausen Seas	Jeffries, M. O., R. Jana, S. Li, and S. McCullars, Antarctic Journal of the US, 30(1-4), 18-21, 1995	n.a.
RD-18	Snow on Antarctic sea ice	Massom, R. A., et al., Reviews in Geophysics, 39(3), 413-445, 2001	n.a.
RD-19	Antarctic sea ice thickness and snow-to-ice conversion from atmospheric reanalysis and passive microwave snow depth	Maksym, T., and T. Markus, Journal of Geophysical Research, 113, C02S12, doi:10.1029/2006JC004085, 2008	n.a.
RD-20	AMSR-E/Aqua L1A Raw Observation Counts	Japan Aerospace Exploration Agency (JAXA), 2003, updated daily. Version 3. June, 2002 - October, 2011. Boulder, Colorado USA: NASA DAAC at the National Snow and Ice Data Center. http://dx.doi.org/10.5067/AMSR-E/AMSREL1A.003.	v03
RD-21	SSM/I sea ice remote sensing for mesoscale ocean-atmosphere interaction analysis: Ice and Icebergs	Kaleschke, L., C. Lüpkes, T. Vihma, J. Haarpaintner, A. Bochert, J. Hartmann, and G. Heygster. Canadian Journal of Remote Sensing, 27(5), 526– 537, 2001.	n.a.
RD-22	Sea Ice Remote Sensing Using AMSR-E 89 GHz Channels	Spreen, G., L. Kaleschke, and G. Heygster, Journal of Geophysical Research, 113(C2), C02S03, doi: 10.1029/2005JC003384, 2008.	n.a.
RD-23	Polar Stereographic Projection and Grid	National Snow and Ice Data Center (NSIDC), http://nsidc.org/data/polar_stereo/ps_grids.html, accessed Dec 5 2014	

Table 1-1: Reference Documents

1.4 Acronyms and Abbreviations

Acronym	Meaning
AMSR-E	Advanced Microwave Scanning Radiometer aboard EOS
AO	Announcement of Opportunity
ASCII	American Standard Code for Information Interchange
ASIRAS	Airborne Synthetic Aperture and Interferometric Radar Altimeter System
CM-SAF	Climate Monitoring Satellite Application Facility
CRDP	Climate Research Data Package
DMSP	Defence Meteorological Satellite Program
DWD	Deutscher Wetterdienst
ECV	Essential Climate Variable

Acronym	Meaning
Envisat	Environmental Satellite
ESA	European Space Agency
EUMETSAT	European Organisation for the Exploitation of Meteorological Satellites
FCDR	Fundamental Climate Data Record
FOC	Free of Charge
FOV	Field-of-View
FTP	File Transfer Protocol
GB	GigaByte
GCOM	Global Change Observation Mission
H	Horizontal polarization
H+V	Horizontal and vertical polarization
MB	MegaByte
MODIS	Moderate Resolution Imaging Spectroradiometer
n.a.	Not applicable
NetCDF	Network Common Data Format
NSIDC	National Snow and Ice Data Center
OIB	Operation Ice Bridge
OSI-SAF	Ocean and Sea Ice Satellite Application Facility
PI	Principal Investigator
PMW	Passive Microwave
POES	Polar Operational Environmental Satellite
PRF	Pulse Repetition Frequency
RADAR	Radio Detection and Ranging
SAR	Synthetic Aperture Radar
SIC	Sea Ice Concentration
SIRAL	SAR/Interferometric Radar Altimeter
SIT	Sea Ice Thickness
SMMR	Satellite Multichannel Microwave Radiometer
SSM/I	Special Sensor Microwave / Imager
SSM/IS	Special Sensor Microwave / Imager+Sounder
Tb	Brightness Temperature
TB	TeraByte
t.b.d.	To be determined
TM	Thematic Mapper
ULS	Upward Looking Sonar
URL	Uniform Resource Locator
V	Vertical polarization

Table 1-2: Acronyms

2 Snow Depth (SD) from Advanced Microwave Scanning Radiometer (AMSR-E)

2.1 Introduction

This part of the Product User Guide (PUG) provides the entry point to the European Space Agency Climate Change Initiative (ESA CCI) Antarctic Sea Ice Thickness Option snow depth (SD) on sea ice dataset, both from a scientific and a technical point of view. Details of the scientific description of the processing chain and algorithms are however willingly kept out of this PUG, and the interested readers are rather directed to the documents Passive Microwave Snow Depth on Antarctic sea ice assessment [RD-01] and the ANT Snow Depth from Alternative Sources [RD-02]. First evaluation results are also contained in [RD-01].

This is issue 2.0 of the PUG. It is provided along with version 1.1 of the AMSR-E snow depth data set for Antarctic sea ice: SDv1.1. Major improvements compared to SDv1.0 are that file format and naming convention comply to the format used for the ESA CCI SIC and SIT prototype products (see [RD-03]), that daily and monthly data files are available and that all monthly data files contain additional information about sea ice concentration, quality flags, etc., as are detailed below.

In short, the SICCI ANT SD dataset is:

- Daily & monthly gridded SD fields based on Passive Microwave Radiometer measurements;
- Maps of Southern Hemisphere with 12.5 km grid spacing;
- Based on AMSR-E data;
- Daily & Monthly maps of total standard error (uncertainty);
- Built upon the algorithms reviewed and modified in [RD-01].

2.2 Scientific Description of the product

This section gives a summary of the science features of the ANT SD dataset. First we point potential users to the known limitations and caveats which we first describe before we give a recommendation to the user in *italic font.* Note that this version of PUG is written before an extensive validation exercise of the dataset, and that the results described below are based on the investigations and literature review results given in [RD-01; RD-02].

2.2.1 Known limitations and caveats

Users of this dataset should be fully aware of the fact that the general methodology used to retrieve snow depth from AMSR-E brightness temperatures does not differ from the known approach [RD-04 to RD-06].

2.2.1.1 *Using an Empirical approach*

The original algorithm [RD-04 to RD-06] is an empirical one, linearly relating observed SD to brightness temperatures measured at 19 GHz and 37 GHz. The new algorithm is similar – except that the coefficients of linear regression used are solely derived from AMSR-E brightness temperature measurements.

The new SD retrieval algorithm is similar to the original one. This applies in particular to the maximal retrieval SD value which is around 50 cm.

However, the skill and usability of such an empirical approach is for sure limited and is determined in particular by

- representativity and quality of the SD observations used in terms of spatio-temporal coverage and ice types (see 2.2.1.2)
- encountered sea ice type (see 2.2.1.3)
- encountered environmental conditions (see 2.2.1.4)

2.2.1.2 *Representativity*

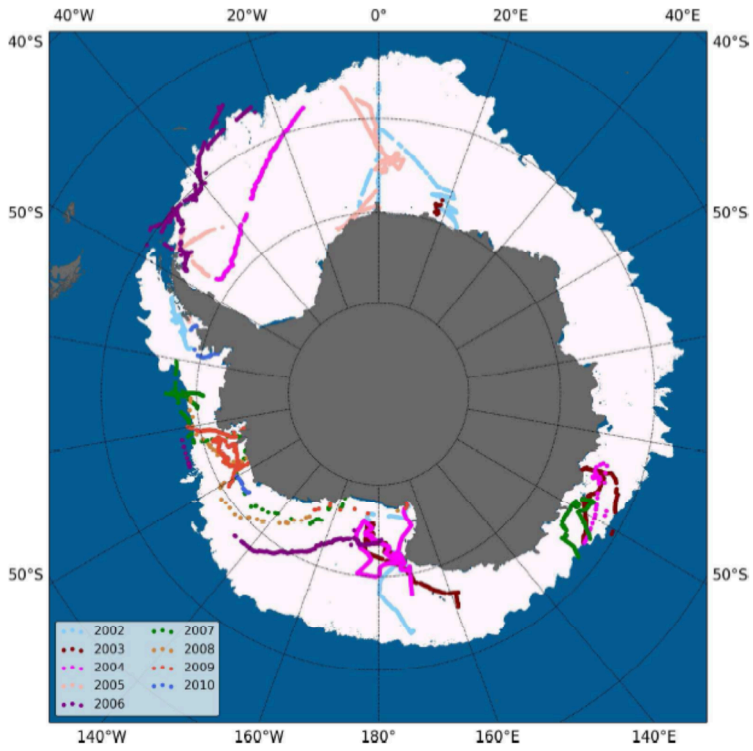

Figure 2.1 ASPeCt ship tracks during 2002-2010 projected onto an AMSR-E sea ice extent map of September 7, 2005 (from [RD-07]).

Figure 2.1 gives the distribution of the ship tracks along which SD observations were carried out which are used to derive the new empirical relationship (see [RD-01]). The map illustrates that large areas of the Antarctic sea ice cover and hence its SD are under-represented in the data set used to derive the empirical approach; we note that also the original algorithm used SD data from a limited region [RD-04]. The similarity of the

results of the inter-comparison between these observations and SSM/I data on the one hand and AMSR-E data on the other hand [RD-01] allows us taking this spatially limited suite of SD observations as the basis for the SD algorithm.

Users should keep in mind though that also the new SD data of the ESA CCI ANT SD v1.1 product could be less representative for snow conditions in some regions while it is more suitable for snow conditions in other regions.

In situ observations of SD are rarely available for months April to July because of the small number of expeditions into the Southern Ocean sea ice cover during that time of the year. The majority of SD data observed in situ is collected during months September to March.

Snow metamorphism caused by melt-refreeze cycles which can occur basically during the entire summer period, i.e. November to February, causes a combination of snow properties and brightness temperatures which are less suitable for the development of the SD retrieval algorithm. Hence the main information for the SD retrieval algorithm development stems from months August to October.

Users should be aware that also the new SD data ESA CCI ANT SD v1.1 product is potentially not suitable for snow conditions of the months outside the winter period April to October and also could potentially be less reliable for months April to June.

The in situ SD observations used to develop the SD retrieval have an accuracy of the magnitude of 5 cm to 10 cm. They are valid for undeformed sea ice. They are not representative for SD on sea ice of the entire sea ice thickness distribution (e.g. [RD-08]). Also, in order to filter out outliers, the new algorithm relies on SD observations which have a low variability on daily temporal and of the magnitude of 100 km spatial scale [RD-01].

Users should keep in mind that also the new SD data ESA CCI ANT SD v1.1 product is potentially less suitable for deformed sea ice.

We note that the three issues mentioned above are not reflected in the SD retrieval uncertainties. These could however be reflected in some way in the SD standard deviation which is provided along with the monthly mean SD data. The SD standard deviation can be taken as a measure of the variability of the SD in the respective grid cell.

2.2.1.3 Sea Ice Types

There is evidence from numerous publications that SD retrieval based on satellite microwave radiometry under-estimates the actual snow depth in areas of deformed sea ice [RD-08 to RD-11]. It can be expected that the same applies to the ESA-CCI ANT SD v1.0 data set; this is reflected in the partly poor agreement of SD observations and ESA-CCI ANT SD v1.1 data in the sea ice regions of the Eastern Antarctic [RD-01].

The new algorithm has not been improved with regard to the documented under-estimation of SD over deformed sea ice.

The new algorithm utilizes the gradient ratio of the 37 GHz and 19 GHz channel vertically polarized brightness temperatures (GR3719) – similar to [RD-04]. Hence the algorithm cannot be used over multiyear ice.

Users should be aware of the fact that even though the classical multiyear ice, as is typical for the Arctic, does not exist in the Southern Ocean, the ESA CCI ANT SD v1.1 product could be biased over old or perennial ice, as occurs in the Weddell Sea, in the Bellingshausen/Amundsen Sea and sometimes also can occur all around Antarctica.

The gradient ratio GR3719 is primarily influenced by the fraction of sea ice. This influence is corrected for before the snow depth is computed. Further, SD is not computed for sea ice concentrations below 20%. Despite these precautions negative SD values exist in areas of reduced sea ice concentrations. These areas are also characterized by an elevated SD retrieval uncertainty.

In the daily SD maps of ESA CCI ANT SD v1.1 product negative SD values – which occur primarily along the ice edge – are *not flagged* out. In these areas usually the SD retrieval uncertainty exceeds 0.5 m.

In the daily SD files of the ESA CCI ANT SD v1.1 product neither an ice concentration nor a quality flag map pointing to these negative SD values is included. In order to avoid being confused by negative SD values and/or very large SD retrieval uncertainties we recommend:

- *Do not use any negative SD values.*
- *Do not use any SD-values for which the ratio |SD uncertainty| / |SD| is larger than 1.*

In the monthly SD maps of the ESA CCI ANT SD v1.1 product negative SD values – which occur primarily along the ice edge – are *flagged* out. Hence the monthly mean SD map does not cover the entire sea ice covered area. This can be seen by, e.g. comparing the SD map with the map of the monthly mean sea ice concentration which is provided along with the SD. This can also be seen by the additional maps included in the monthly product: number of days with negative SD in the respective grid cell; number of days with valid data for computation of the monthly mean sea ice concentration; number of days with valid, e.g. positive SD values, for computation of the monthly mean SD.

2.2.1.4 Environmental conditions

Snow properties are known to vary a lot on Antarctic sea ice [RD-12 to RD-18]. Some of these, e.g. the snow density, the snow grain size and the snow wetness influence SD retrieval using microwave radiometry [RD-04; RD-19]. These properties can either change directly at the snow surface, e.g. due to direct atmosphere-snow interaction like snow fall or rain on snow or surface melt. These can however also change due to more complex atmosphere-snow-sea ice-ocean interaction, e.g. due to flooding of the ice-snow interface with sea water because of a too heavy snow load and subsequent re-freezing of the flooded snow layer. All these influence the accuracy of the SD product.

Neither the actual variations in the atmospheric conditions nor in the snow properties are known. Therefore, these variations cannot be included in the uncertainty estimation and hence the SD retrieval uncertainties do not show elevated values in case environmental conditions are exceptional. However, in the monthly ESA CCI ANT SD v1.1 product files the SD standard deviation within the respective month is given for every grid cell. This standard

deviation can be taken as a measure of the temporal variability of the SD in the respective month and grid cell. High variability can be caused by both actual variations in SD due to continued snow accumulation on sea ice but also by artificial variations in SD due to weather-induced changes in snow properties, e.g. grain size.

Users should be careful with interpretation of SD values in areas of large SD variability and should be especially alerted by sudden drops in SD during the freezing period.

2.2.2 Description of the algorithm

In this section, we highlight the features of the SD processing [RD-01].

AMSR-E L1A Raw Observation Count data (Version 3), provided by the NSIDC (http://nsidc.org/data/amsrel1a, [RD-20]) are used to derive the brightness temperature gradient ratio GR3719 (henceforth GRV) and to compute the sea ice concentration using the ARTIST Sea Ice (ASI) algorithm [RD-21; RD-22]. Daily averages are computed from the swath data. Brightness temperatures are not corrected for atmospheric influence.
New regression coefficients for the empirical relation between SD observations (collocated ASPeCt ship-based SD observations) and GRV were derived following [RD-04]. For this purpose new open water tie points based on AMSR-E data are required and computed. They are 184.7 K $\pm$ 0.7 K for the 18.7 GHz channel and 210.5 K $\pm$ 0.8 K for the 36.5 GHz channel and kept fixed for the entire AMSR-E period. The resulting values for GRV were compared with ASPeCt SD observations for the winter months (April to October) by means of linear regression analysis. For the derivation of the final set of regression coefficients the following constrains were applied:

1. The uncertainty of the GRV - SD pairs had to be < 0.004 for GRV.
2. The ratio of the observed (ASPeCt) mean, daily along-track SD to its standard deviation had to be < 0.3.
3. Three artificial regression points were added at SD = 0 cm and GRV values 0.004, 0.005 and 0.006 to include GRV for thin bare sea ice.

The resulting regression equation which is used for the SD retrieval is:

$$S_{ASPeCt} = (-864 \pm 131)\ \text{cm} \cdot GRV + (5.4 \pm 2.1)\ \text{cm} \qquad (2.1)$$

The calculated uncertainties represent the 1σ-standard deviation of the fit. The correlation coefficient is -0.87. Compared to the old regression coefficients for AMSR-E (slope: -782 cm, y-intercept: 2.9 cm) the slope is only slightly lower but the y-intercept did significantly increase.

The SD uncertainty is computed using Gaussian error propagation. The input uncertainties of the fit are given in the equation above. The input uncertainties of the GRV are derived based on the noise of the brightness temperatures and the theoretical uncertainty of the ASI sea ice concentration [RD-22]. Hence the ESA CCI ANT SD v1.1 dataset comes with uncertainty estimates for every grid cell with a SD value. All uncertainties are intended as one standard deviation around the provided SD value (acting as the mean of the distribution).

The retrieval of SD and SD uncertainty is carried out on a swath-by-swath basis. Subsequently daily averages are computed and form the ESA CCI ANT SD v1.1 data set.

The daily gridded snow depth and snow depth uncertainty products are then used to calculate the monthly mean snow depth, the monthly snow depth uncertainty and the snow depth variability.

Here, the snow depth within one pixel only represents the sea ice covered fraction of this pixel. In the monthly mean snow depth this is considered by weighting the snow depth pixel value by sea ice concentration

$$\bar{S} = \frac{\sum_{i=1}^{N} C_i S_i}{\sum_{j=1}^{N} C_j} \qquad (2.2)$$

where S_i is the daily averaged snow depth, C_i is the daily averaged sea ice concentration, and N is the number of days contributing to the monthly average. Here, to calculate the monthly snow depth average the daily averaged ASI sea ice concentration [RD-21; RD-22] is used (University of Bremen; http://www.iup.uni-bremen.de:8084/amsr/amsre.html). The sea ice concentration product has a grid resolution of 6.25 km x 6.25 km. Since the snow depth product is provided at 12.5 km x 12.5 km grid resolution the resolution of the sea ice concentration is reduced to 12.5 km x 12.5 km beforehand.

The monthly snow depth uncertainty is then calculated via

$$\sigma_{S,err} = \pm \sqrt{\sum_{i=1}^{N} \left(\frac{C_i \sigma_{S,i}}{\sum_{j=1}^{N} C_j} \right)^2 + \sum_{i=1}^{N} \left(\frac{S_i \sum_{j=1}^{N} C_j - \sum_{k=1}^{N} C_k S_k}{(\sum_{l=1}^{N} C_l)^2} \sigma_{C,i} \right)^2} \qquad (2.3)$$

where $\sigma_{S,i}$ is the uncertainty of the daily snow depth average, $\sigma_{C,i}$ is the uncertainty of the sea ice concentration estimated from Figure 9 in Spreen et al. [RD-22]. The sea ice concentration uncertainty is estimated from the figure in 10% intervals (except for 100%) and is given in Table 2.1.

Table 2.1 Sea ice concentration uncertainties estimated from Fig. 9 in Spreen et al. [RD-22].

C [%]	σ [%]
20 - 29	21
30 - 39	19
40 - 49	16
50 - 59	13
60 - 69	11
70 - 79	9
80 - 89	7.5
90 - 99	7
100	6

The snow depth variability is calculated from the snow depth averages and the daily snow depth averages via

$$\sigma_{S,var} = \sqrt{\frac{\sum_{i=1}^{N} (S_i - \bar{S})^2}{N - 1}} \qquad (2.4)$$

where $\bar{S}$ is the monthly averaged snow depth according to Eq. 2.2.

2.3 Technical description of the product

In this section, the SD product files are described in terms of content, file name, data format, grid, and others.

2.3.1 Example

To support the reading of the technical specifications, we start this section by providing an example of the SD (Figure 2.2) and the SD retrieval uncertainty (Figure 2.3) for Sep. 7 2005.

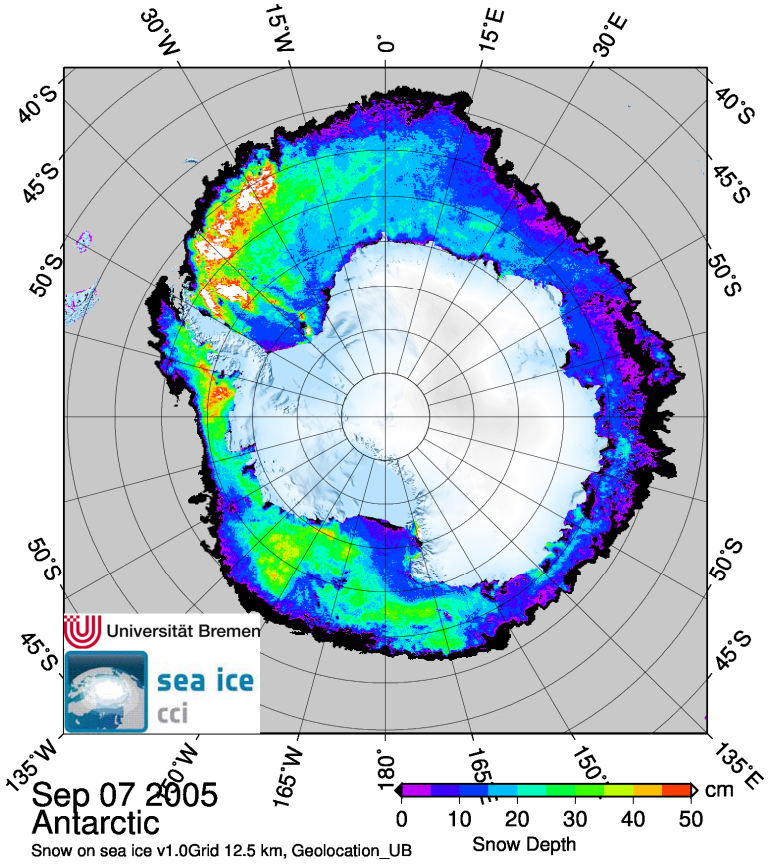

Figure 2.2 Map of the daily snow depth distribution for Sep. 7 2005 in the Southern Ocean. Regions with negative snow depths are given in black. Sea ice areas where the snow depth exceeds the theoretically possible upper limit of the snow depth of around 50 cm are shown in white.

Figure 2.2 shows the kind of classic distribution of the snow depth on sea ice as can be expected based on the distribution of different ice types. In the northern and north-western Weddell Sea, the southern parts of the Bellingshausen Sea and some areas of the Amundsen and Ross Seas snow depths are relatively large and exceed 30 cm. Regions downstream of major polynyas producing and exporting thin ice northwards, e.g. the Ross Ice Shelf polynya in the Ross Sea and the Filchner-Ronne Ice Shelf polynya in the Weddell Sea show substantially less snow: < 10 cm. The majority of the sea ice enclosing East Antarctica shows snow depths between 5 cm and 20 cm. In these regions deformation might be more wide-spread and hence the

potential that the snow depth is under-estimated might be larger than on the sea ice enclosing West Antarctica.

Figure 2.3 reveals that the daily snow depth retrieval uncertainty is relatively uniform and takes values around 4 cm. Elevated values tend to occur only near the ice edge – except in the Weddell Sea and in some isolated areas in the Bellingshausen / Amundsen Sea where snow depth retrieval uncertainty exceeds 6 cm.

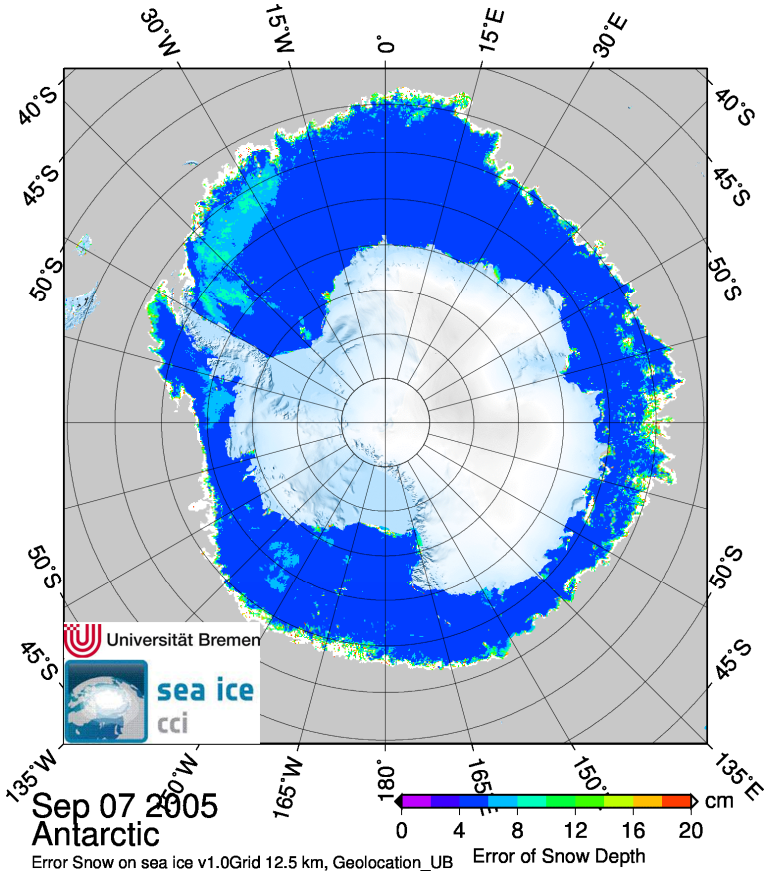

Figure 2.3 Map of the daily snow depth retrieval uncertainty distribution for Sep. 7 2005 in the Southern Ocean. Regions with SD retrieval uncertainty > 20 cm are given in white.

In the next three figures (Figure 2.4 to 2.6) we give examples of the monthly SD distribution, its mean monthly retrieval uncertainty and the SD temporal variability (SD standard deviation) – all for September 2005.

Figure 2.4 shows similar features to those already identified in Figure 2.2. In some areas the monthly mean snow depth seems to be larger than in the daily snow depth map of September 7, 2005, e.g. in some areas around East Antarctica, while in other areas the monthly mean snow depth reveal smaller values than the daily one, e.g. in the eastern Weddell Sea. Note that in contrast to Figure 2.2 negative snow depth values have been set to zero and are hence missing here. Note further, that areas where the algorithm provides snow depths above the threshold of 50 cm are not a daily phenomenon but that such high snow depths tend to be typical for, e.g., the western Weddell Sea and also the southern Bellingshausen Sea. This is in line with findings given in [RD-02]. The monthly data files of the ESA CCI ANT SD v1.1 product contain maps showing the number of days per month

where the snow depth was negative or where the snow depth exceeds 50 cm.

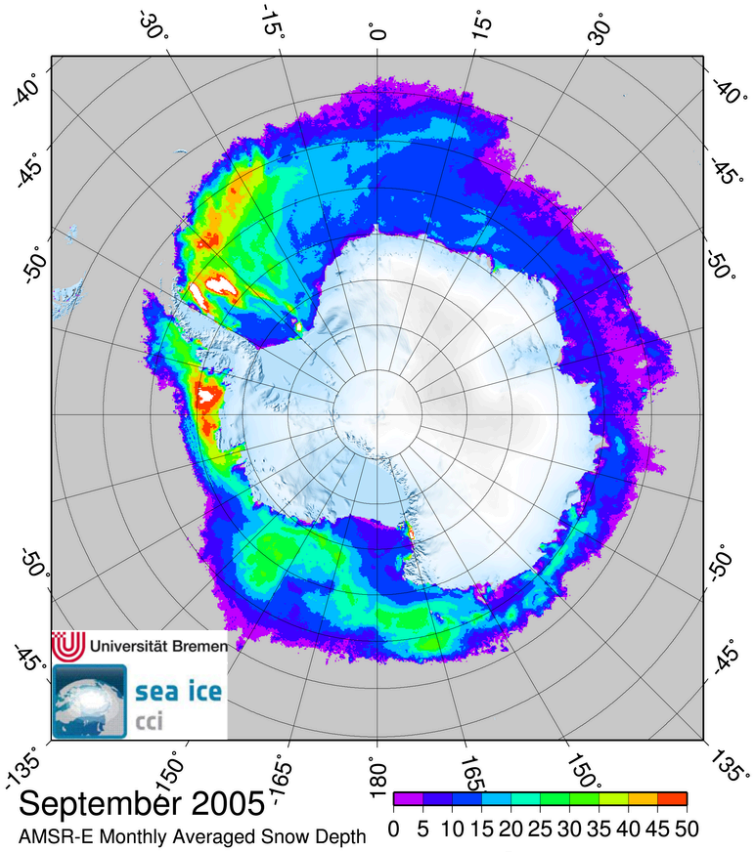

Figure 2.4 Map of the monthly mean snow depth distribution for September 2005 in the Southern Ocean. Regions with negative snow depths are flagged. Snow depth is given in centimetres. Sea ice areas where the mean monthly snow depth exceeds the theoretically possible upper limit of the snow depth of around 50 cm are shown in white.

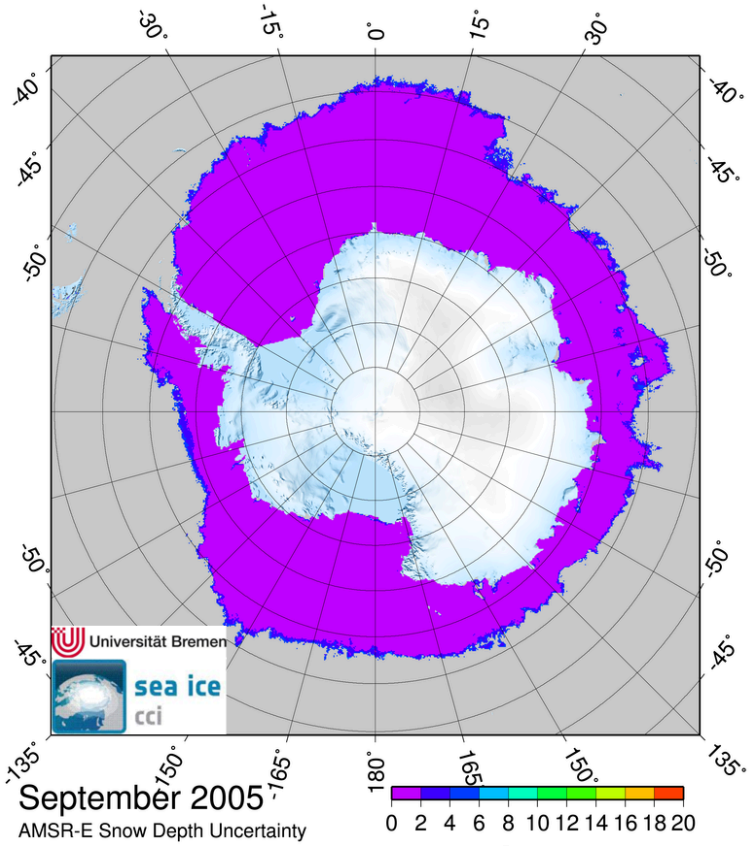

Figure 2.5 Map of the monthly mean snow depth retrieval uncertainty distribution for September 2005 in the Southern Ocean. Regions with negative snow depths are not included. Snow depth uncertainty is given in centimetres.

Figure 2.5 reveals that the average monthly retrieval uncertainty based on uncertainties in the algorithm itself and in the sea ice concentration reduces to values being commonly below 2 cm. However, this uncertainty does not include the potential of the algorithm to provide a bias in the snow depth due to the influencing factors discussed above. In order to give the user a tool at hand to check in which regions the snow depth is quite variable and hence needs to perhaps interpreted more carefully than in other regions, a map of the monthly snow depth standard deviation is provided for each month in addition, such as is shown in Figure 2.6. This map reveals that indeed the snow depth standard deviation is larger than the retrieval uncertainty but that the difference is within 2 cm for most of the area for September 2005. There are, however, many regions where the snow depth standard deviation is substantially larger than the retrieval uncertainty such as in the Bellingshausen Sea, the western Ross Sea and the north-western Weddell Sea. While some of these variations might be real some of these might be artificial due to snow property effects on snow depth retrieval.

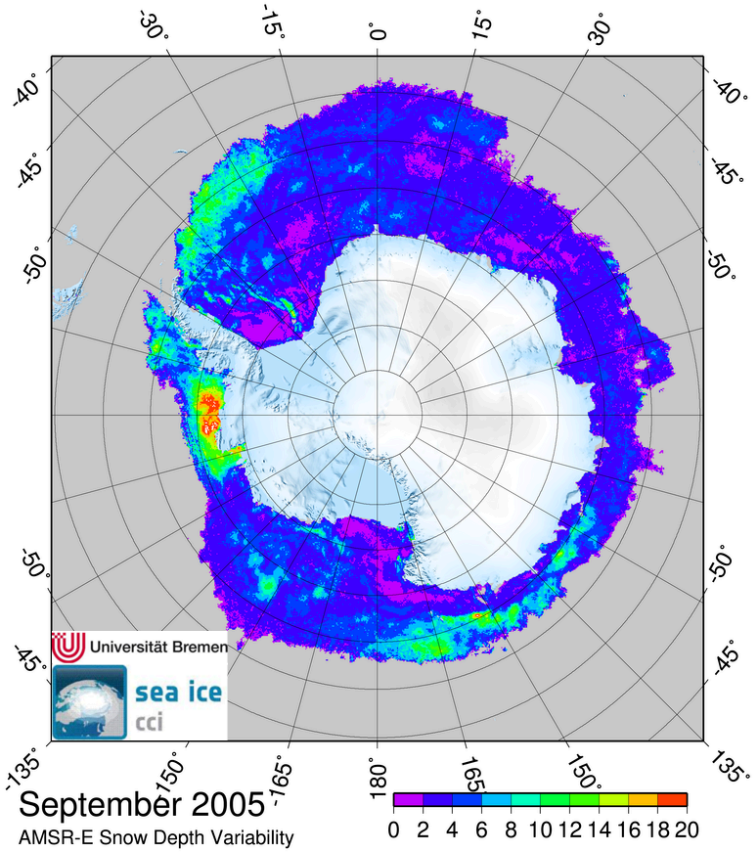

Figure 2.6 Map of the snow depth standard deviation distribution for September 2005 in the Southern Ocean. Regions with negative snow depths are not included. Snow depth standard deviation is given in centimetres.

2.3.2 Content of product files

The distributed product files are so called "Level 4" files that are daily and monthly gridded maps of snow depth (SD) and SD retrieval uncertainties for the Southern Hemisphere. Each map has dimension 632 (x-coordinate, number of columns) times 664 (y-coordinate, number of rows). Each file contains:

- Latitude and longitude for each grid point. Name of the variable is Latitude and Longitude. These are based on the NSIDC grid with 12.5 km x 12.5 km grid resolution, in degrees north and degrees east, respectively

- A map of analysed, daily or monthly averaged snow depth. Name of the variable is SNOW_DEPTH or MONTHLY_AVERAGED_SNOW_DEPTH. This variable has the unit m and provides a snow depth estimate wherever the mean daily or monthly sea ice concentration is > 20% (as derived with the ASI algorithm (see above). Negative SD values are not flagged in the daily product. Negative SD values are set to zero in the monthly product.

- A map of daily or monthly snow depth retrieval uncertainties. Name of the variable is SNOW_DEPTH_UNCERTAINTY. This variable has the unit

m and provides an estimate of the snow depth retrieval uncertainty for every grid cell with a valid snow depth value (see above).

Each monthly data product file contains in addition:

- A map of the snow depth standard deviation for the respective month. The name of the variable is SNOW_DEPTH_VARIABILITY. This variable has unit m and provides a measure of the temporal variability of the snow depth for every grid cell. All non-negative daily snow depth values of the respective month are considered.

- A map of the monthly mean sea ice concentration derived from ASI algorithm daily sea ice concentration estimates. This variable is MONTHLY_AVERAGED_SEA_ICE_CONCENTRATION and has unit %.

- A map of the occurrence of negative daily SD values. The name of the variable is NUMBER_OF_NEGATIVE_SNOW_DEPTH. It has no units and simply counts the number of days for which at the respective grid cell in the respective month the daily SD values is negative.

- A map of the occurrence of daily SD values above 50 cm. The name of the variable is NUMBER_OF_SNOW_DEPTHS_GT_50_CM. It has no units and simply counts the number of days for which at the respective grid cell in the respective month the daily SD values is above 50 cm.

- A map of the number of days with valid daily sea ice concentration data. The name of the variable is NUMBER_OF_DAYS_FOR_SEA_ICE_CONCENTRATION_AVERAGE. It has no units and counts the number of days for which at the respective grid cell in the respective month a valid daily sea ice concentration value exists. This map can also serve as the land distribution map.

- A map of the number of days with valid daily snow depth data. The name of the variable is NUMBER_OF_DAYS_FOR_SNOW_DEPTH_AVERAGE. It has no units and counts the number of days for which at the respective grid cell in the respective month a valid, i.e. non-zero, daily SD value exists.

2.3.3 Temporal coverage

The daily data set is available in the ESA CCI ANT SD v1.1 product for the entire AMSR-E period: from June 19, 2002, to October 4, 2011. The monthly data set is available from June 2002 to September 2011.

Temporal resolution is daily and monthly.

2.3.4 Product grid and geographic projection

The SD datasets is (still) delivered on the NSIDC polar-stereographic grid [RD-23] and not on the EASE grid v2.0 as the other ESA SICCI products.

Grid center is the South Pole. The tangential plane is located at 70degS. The grid is not symmetric around to pole along axis given by the 0degE / 180degE meridians but is covering 32 more rows in the direction centered at the 0degE meridian. The grid coordinates are given in Table 2.1.

Dimensions	X [km]	Y [km]	Latitude [deg N]	Longitude [deg E]
X: 632 Y: 664 X1 … X632: 7900 km Y1 … Y664: 8300 km	-3950	4350	-39.2979	317.7633
	0	4350	-51.3757	0.0000
	3950	4350	-39.2979	42.2367
	3950	0	-54.7095	90.0
	3950	-3950	-41.5152	135.0
	0	-3950	-54.7095	180.0
	-3950	-3950	-41.5152	225.0
	-3950	0	-54.7095	270.0

Table 2.2: Definition of the Southern Hemisphere grid used for the Snow Depth dataset.

2.3.5 Convention for file names

The ESA CCI ANT SD v1.1 dataset widely follows the ESA-CCI convention for file names. The daily files are named

ESACCI-SEAICE-L4-SNOWDEPTH-AMSR-SH12kmNSIDCPOLSTEREO-<YYYYMMDD>-fv01.01.nc

where <YYYYMMDD> denotes the date string with YYYY for the year, e.g. 2002, MM for the month, i.e. 06, and DD for the day, i.e. 19. <SH12kmNSIDCPOLSTEREO> stands for Southern Hemisphere, NSIDC polar-stereographic grid with 12.5 km grid resolution.

The monthly files are named

ESACCI-SEAICE-L4-SNOWDEPTH-Monthly-Mean-AMSR-SH12kmNSIDCPOLSTEREO-<YYYYMMDD>-fv01.01.nc

2.3.6 File format

The Snow Depth datasets are netCDF files following convention CF1.6.

All variables are stored a short (16 bit) integer except the coordinates which are stored as double precision floating point (double).

2.3.7 Access to data

The Snow Depth dataset can be accessed via:

- http://icdc.zmaw.de/projekte/esa-cci-sea-ice-ecv0.html
- http://www.iup.uni-bremen.de:8084/amsredata/AMSRE_Snow_Netcdf/

2.3.8 Dataset version history

v1.1: This version.

v1.0: Basic first release; only daily SD and SD uncertainty estimates, no monthly values; files not following CF-convention; no further information such as flags and sea ice concentration included.

< End of Document >